THE JOURNAL OF BIOLOGICAL CHEMISTRY
Vol. 272, No. 34, Issue of August 22, pp. 21233–21239, 1997
Printed in U.S.A.

Dimerization Interactions of the *b* Subunit of the *Escherichia coli* F_1F_0-ATPase*

(Received for publication, April 17, 1997, and in revised form, May 20, 1997)

Derek T. McLachlin‡ and Stanley D. Dunn§

From the Department of Biochemistry, University of Western Ontario, London, Ontario, N6A 5C1 Canada

Site-directed mutagenesis and N-terminal truncations were used to examine dimerization interactions in the *b* subunit of *Escherichia coli* F_1F_0-ATPase. Individual cysteine residues were incorporated into b_{syn}, a soluble form of the protein lacking the membrane-spanning N-terminal domain, in two main areas: the heptad repeat region and the hydrophobic region which begins at residue Val-124. The tendencies of these cysteine residues to form disulfide bonds with the corresponding cysteine in the b_{syn} dimer were tested using disulfide exchange by glutathione and air oxidation catalyzed by Cu^{2+}. Within the heptad repeat region, only cysteines at residues 59 and 60, which occupy the *b* and *c* positions of the heptad repeat, showed significant tendencies to form disulfides, a result inconsistent with a coiled-coil model for b_{syn}. Mixed disulfide formation most readily occurred with the S60C + L65C and A61C + L65C pairs. Cysteines at positions 124, 128, 132, and 139 showed strong tendencies to form disulfides with their mates in the dimer, suggesting a parallel α-helical interaction between the subunits in this region. Deletion of residues N-terminal to either Glu-34 or Asp-53 had no apparent effect on dimerization as determined by sedimentation equilibrium, while deletion of all residues N-terminal to Lys-67 produced a monomeric form. These results imply that residues 53–66 but not 24–52 are essential for b_{syn} dimerization. Taken together the results are consistent with a model in which the two *b* subunits interact in more than one region, including a parallel alignment of helices containing residues 124–139.

The F_1F_0-ATP synthase, or ATPase, is responsible in oxidative phosphorylation and photophosphorylation for the translocation of protons across a membrane with concomitant synthesis of ATP. The enzyme complex consists of a membrane-spanning sector (F_0) that conducts protons, and a membrane-peripheral sector (F_1) that uses energy from proton movement to synthesize ATP (for reviews, see Refs. 1–4). The mechanism by which energy coupling from F_0 to F_1 takes place is currently under intense investigation.

In *Escherichia coli*, the F_0 sector is composed of three different subunits of stoichiometry ab_2c_{9-12}; the two *b* subunits are believed to exist as a dimer. The *a* and *c* subunits appear to be directly involved in proton movement across the membrane, while *b* is not. The arrangement of the F_0 subunits within the membrane is uncertain; some believe that the *c* subunits are clustered together with *a* and *b* on the periphery (5–7) while others propose that *a* and the two *b* subunits are surrounded by a ring of *c* subunits (8, 9). *b* has a single transmembrane region at its N terminus; the remainder of the 156-residue protein is hydrophilic with the exception of a short stretch of hydrophobic amino acids at residues 124–132. Based on its sequence the protein is predicted to be largely α-helical in nature, and a heptad repeat has been discerned between residues 33 and 79, suggestive of a coiled-coil interaction in this region. Previously one of us has constructed a gene encoding the hydrophilic portion of *b* (10). The product of this gene, b_{sol}, is soluble, forms a dimer in solution, is mostly α-helical as measured by circular dichroism, and competes with the F_0 sector for binding to F_1. Therefore it is likely that b_{sol} adopts a structure similar to the hydrophilic region of full-length *b*.

Proteolysis studies have shown that the hydrophilic portion of *b* is required for the binding of F_1 to the membrane (11–13), and mutation of the glycine at position 131 to aspartate prevents proper assembly of the F_1F_0 complex (14). Therefore the *b* subunit provides a critical link between the two sectors, but its role in energy transduction has yet to be determined.

Two regions of *b* have been suggested to play a role in its dimerization: the heptad repeat region (residues 33–79; Ref. 10) and the hydrophobic region near the C terminus (residues 124–132; Ref. 15). To investigate these regions, and to obtain information about their relative orientation, we have introduced individual cysteine mutations into the soluble hydrophilic portion of *b*. By estimating the relative propensities of cysteines introduced at various positions to form an intersubunit disulfide bond, one may gain insight as to the proximity of the residues. In addition, several forms of *b* that have been truncated at the N terminus were analyzed by ultracentrifugation to clarify the role of the N-terminal region in dimerization.

EXPERIMENTAL PROCEDURES

Plasmid Construction and Mutagenesis—Molecular biological techniques were performed essentially as described in Sambrook *et al.* (16). Strain JM103 of *E. coli* (17) was used as the host for plasmids based on pUC8. Strain MM294 was used as the host for plasmids based on pSD80. The *uncF* strain KM2 (18), generously provided by Kimberly McCormick and Brian Cain, is based on strain 1100 and was used for expression of full-length *b* constructs.

To construct the gene encoding b_{syn}, four pairs of overlapping single-stranded synthetic oligonucleotides were made double-stranded by annealing and subsequent treatment with Klenow fragment. The oligonucleotides were inserted one at a time into the multiple cloning region of pUC8 (19) to produce pDM3. The sequence of the gene was verified by DNA sequencing using the Sanger method.

Cysteine mutations were incorporated into pDM3 by two different methods. In some cases, degenerate oligonucleotides with the potential to encode mutations at several sites were synthesized and incorporated into the plasmid. For other mutations, mutagenic primers were used

* The work was supported in part by Grant MT-10237 from the Medical Research Council of Canada. The Beckman XL-A analytical ultracentrifuge was acquired through support from the Academic Development Fund of the University of Western Ontario. The costs of publication of this article were defrayed in part by the payment of page charges. This article must therefore be hereby marked "*advertisement*" in accordance with 18 U.S.C. Section 1734 solely to indicate this fact.

‡ Supported by a Postgraduate Scholarship from the Natural Sciences and Engineering Research Council of Canada and an Ontario Graduate Scholarship.

§ To whom correspondence should be addressed. Tel.: 519-661-3055; Fax: 519-661-3175; E-mail: sdunn@julian.uwo.ca.

along with either the forward or reverse M13/pUC sequencing primer in polymerase chain reactions; the polymerase chain reaction products were incorporated into pDM3 using appropriate restriction enzymes. The resulting *E. coli* transformants were screened for expression of b_{syn} containing cysteine as described previously (20). DNA sequencing by the Sanger method was used to verify the sequence of the entire mutagenic insert.

Plasmid pSD80 (21) carries a *tac* promoter upstream of the multiple cloning site, an *unc* transcription terminator downstream of the *Hin*dIII site at the end of the multiple cloning region, and the $lacI^q$ gene elsewhere on the plasmid. The single *Msc*I site of pSD80 was removed by cutting with that enzyme and ligating an *Xba*I linker into the site to produce plasmid pSD82, which served as the basis for pSD100.

The *unc* sequence inserted in pSD51 (10) spans residues A-2144 through C-2940, numbered as in Ref. 22, beginning 43 bases upstream from *uncF*, which encodes *b*, and extending about halfway through the next gene, *uncH*. Polymerase chain reaction mutagenesis was used to amplify this entire insert from pSD51 and to introduce a translation initiation region and an *Msc*I restriction site upstream of the *unc* region. The product was cloned into pSD82, using the *Eco*RI and *Hin*dIII site to yield plasmid pSD84. Subsequent replacement of part of the non-*unc* upstream sequence with a synthetic double-stranded fragment gave plasmid pSD100, which contains the following sequence beginning at the *Eco*RI cloning site: GAATTCT**GGAGG**ATTTTAAA**ATG**TCTTACTGGCCAGAGCTCGGTACCC. Within this segment are a Shine-Dalgarno sequence and a start codon (both shown in bold) for a peptide beginning with amino acid sequence MSYWPELGT. Within the sequence encoding the peptide is a series of sites specific for restriction endonucleases *Msc*I, *Sac*I, and *Kpn*I. The *Msc*I site (underlined), which was used extensively in subsequent work, spans the codons for the tryptophan and proline residues. The sequence shown is linked to *unc* residue A-2144 located upstream from the *uncF* start codon.

Plasmid pSD100 was originally designed for the production of plasmids encoding N-terminal deletions of *b* through the use of exonuclease III. In the current work, however, it was used for two different purposes. First, the *Msc*I and *Hin*dIII sites were used for subcloning of segments of *uncF* to produce plasmids pKK1, pSD111, and pSD114, which have in-frame fusions between the leader sequence and the inserted *uncF* sequence. In the construction of plasmid pKK1, which encodes protein b_{65-156}, the 578-base pair *Pvu*II-*Hin*dIII fragment of pSD59 (10) was inserted. The 322-base pair insert used for the construction of pSD111, which encodes protein b_{53-156}, was obtained by cutting pDM3 with *Bgl*II, filling the end with Klenow fragment, then cutting with *Hin*dIII. The 373-base pair fragment used for the construction of pSD114, which encodes protein b_{34-156}, was obtained by cutting pDM3 with *Mfe*I, removing overhanging bases with mung bean nuclease, then cutting with *Hin*dIII. Constructs were verified by restriction enzyme mapping and, for pSD111 and pSD114, sequencing through the site of the in-frame fusion. The protein products were shown to be recognized by *b*-specific monoclonal antibodies.

Second, the plasmid pDM8, expressing the entire *b* subunit, was generated by subcloning the *Sna*BI-*Hin*dIII fragment of pDM3 into pSD100. Thus pDM8 carries the wild type *uncF* gene sequence from the initiation codon to the *Sna*BI site, and the synthetic gene sequence from the *Sna*BI site to the termination codon. The mutations R138C and S139C were subcloned individually from their pDM3-like plasmids into pDM8 using the *Ngo*AIV and *Hin*dIII sites of the synthetic gene; the resulting plasmids were called pDM112 and pDM113, respectively.

Protein Purification—The expression and purification of b_{syn} was carried out essentially as described earlier for b_{sol} (10), with the exception of the final stage. In this step, the protein was loaded onto a column of DEAE-Sepharose instead of a column of Sephacryl S-300, and was eluted with a linear gradient of 0–250 mM NaCl in 250 ml of 25 mM imidazole-HCl, pH 6.4, 1 mM EDTA. The resulting column fractions containing b_{syn} were typically pooled, concentrated using an Amicon Diaflo apparatus with a YM-10 membrane, dialyzed against 50 mM Tris-HCl, pH 8.0, 1 mM EDTA, and stored at −80 °C. Purification of mutant proteins containing cysteine was identical except that 1 mM dithiothreitol (DTT)[1] was added to all buffers after the 40% $(NH_4)_2SO_4$ precipitation step.

Protein b_{34-156}, which is expressed from plasmid pSD114, was purified by procedures similar to those used for b_{syn}, except that the protein was precipitated with 45% saturated ammonium sulfate, and size exclusion chromatography on a column of Sephacryl S-200 was added as a final step. Protein b_{53-156}, which is expressed from plasmid pSD111, was purified by procedures similar to those used for b_{syn}, except that the protein was precipitated with 45% saturated ammonium sulfate, and that this was followed by a pH precipitation at pH 5.1 before DEAE-Sepharose chromatography. The precursor of protein b_{67-156}, which was expressed from plasmid pKK1, was found in the pellet from the initial ultracentrifugation. The pellet was resuspended in buffer containing 50 mM Tris-HCl, pH 8.0, 10 mM $MgCl_2$, stored at 4 °C overnight, and the ultracentrifugation was repeated. Analysis of the supernatant and pellet fractions by SDS-PAGE revealed the protein to have been completely solubilized, but with a slight increase in electrophoretic mobility. The protein was precipitated with 90% saturated ammonium sulfate, then purified by ion exchange chromatography on DEAE-Sepharose and size exclusion chromatography on Sephadex G-75. The protein was followed by SDS-PAGE and by absorbance at 230 nm, as it lacked absorbance at 280 nm.

Disulfide Bond Formation Induced by Glutathione (GSH)—Oxidized and reduced glutathione were purchased from Sigma. Samples of the proteins to be tested were converted to the fully oxidized form by dialysis at 4 °C for 24 h in buffer containing 0.1 M $NaHCO_3$ and 10 μM $CuCl_2$. The buffer was then changed by dialysis to 0.1 M Tris-HCl, pH 7.5, 0.1 M NaCl, 1 mM EDTA (glutathione reaction buffer, GRB). Other samples, to be tested in parallel, were not oxidized with $CuCl_2$ but were converted to the fully reduced form by dialysis into GRB containing 1 mM DTT. The protein concentrations of all samples were measured by the Bradford assay (23), and were adjusted to a uniform level (usually in the range of 0.5–1.0 mg/ml or 32–64 μM). In cases where two proteins containing different mutations were used, the proteins were first adjusted to the same concentration, and then equal volumes were mixed. To the pre-oxidized samples were added 2 volumes of a glutathione mixture containing 13 mM GSSG and 12 mM GSH. To the pre-reduced samples were added 2 volumes of a mixture containing 13.75 mM GSSG and 11.25 mM GSH. The different ratios of GSSG:GSH allow for reduction of GSSG by the 1 mM DTT present in the pre-reduced samples; the final ratios were identical at GSSG:GSH = 1.08:1. The reactions were incubated at room temperature. At various time points (*e.g.* 30 min, 1 h, 2 h, and 4 h), 15-μl aliquots were quenched with 10 μl of 0.1 M *N*-ethylmaleimide (NEM), diluted into SDS-PAGE sample buffer lacking reducing agent, and heated to 100 °C for 5 min. A zero time point was prepared by quenching an aliquot before the glutathione mixtures had been added. All samples were analyzed on SDS-PAGE under nonreducing conditions.

Disulfide Bond Formation Induced by Air Oxidation Catalyzed by Cu^{2+}—The concentrations of purified or partially purified proteins were adjusted to uniformity (typically 0.5–1.0 mg/ml) with 50 mM Tris-HCl, pH 8.0, 1 mM EDTA, 1 mM DTT. The partially purified proteins had been purified up to and including the 40% $(NH_4)_2SO_4$ precipitation stage (see Ref. 10). The proteins were dialyzed at 4 °C in 1 liter of 50 mM Tris-HCl, pH 8.0, 1 mM EDTA, 1 mM DTT overnight. As a zero time point, 5-μl aliquots were then added to 45 μl of SDS-PAGE sample buffer containing 15 mM NEM and heated to 100 °C for 5 min. The dialysis bags were transferred to 1 liter of 0.1 M $NaHCO_3$, 10 mM cysteine, 10 μM $CuCl_2$; in some cases the cysteine was omitted. The bicarbonate buffer was always prepared immediately before use. Five-μl aliquots were taken and quenched as described above after 2, 4, 6, 8, 24, and 48 h of dialysis, then analyzed by non-reducing SDS-PAGE. Results obtained by this procedure were similar to those seen with the GSH/GSSG method provided the free cysteine was present; in its absence all mutant proteins containing cysteine residues exhibited essentially complete disulfide formation after 24 h. Substitution of 0.1 M Tris-HCl, pH 7.5, 0.1 M NaCl for the 0.1 M $NaHCO_3$ did not affect the results obtained.

Expression of Full-length b and Partial Purification of Membranes—*E. coli* KM2 bearing pDM112 or pDM113 was grown in 1 liter of Luria broth at 37 °C with shaking. When A_{600} reached 0.060, isopropyl β-D-thiogalactopyranoside was added to 15 μM, and growth was continued until A_{600} reached 0.800. The cells were harvested by centrifugation, washed with 50 mM Tris-HCl, pH 8.0, 10 mM $MgCl_2$, and stored at −80 °C. The cells were resuspended in a volume of 50 mM Tris-HCl, pH 8.0, 10 mM $MgCl_2$, 1 mM phenylmethylsulfonyl fluoride equal to 10 times their packed wet weight, then disrupted by passage through a French pressure cell at 20,000 p.s.i. After centrifugation for 10 min at 10,000 rpm in a Beckman JA-20 rotor, the supernatant was centrifuged for 2 h at 38,000 rpm in a Beckman Ti-50 rotor. The pellet was resuspended in 10 mM triethanolamine-H_2SO_4, pH 7.5, 10 mM EDTA, 10% glycerol and centrifuged at 38,000 rpm as before. The pellet was resuspended in 50 mM triethanolamine-HCl, pH 7.5, 5 mM $MgCl_2$, 10%

[1] The abbreviations used are: DTT, dithiothreitol; GSH, reduced glutathione; GSSG, oxidized glutathione; GRB, glutathione reaction buffer; NEM, *N*-ethylmaleimide; PAGE, polyacrylamide gel electrophoresis.

glycerol, and centrifuged as before. The pellet was then resuspended in 0.5 ml of 50 mM triethanolamine-HCl, pH 7.5, 5 mM $MgCl_2$, 10% glycerol and stored at −80 °C. *E. coli* 1100 cells were treated in the same manner; the level of induction used results in expression of *b* from the plasmids at a level approximately equal to the level of chromosomal *b* expression in 1100, as determined by Western blotting (data not shown).

Disulfide Bond Formation in Partially Purified Membranes—Protein concentrations of membrane samples from 1100, KM2/pDM112, and KM2/pDM113 were measured by the method of Lowry *et al*. (24). The concentrations were adjusted to 2.0 mg of total protein per ml, and then $CuCl_2$ was added to a concentration of 10 μM. The mixture was allowed to stand in an open container at 4 °C, and periodically (1, 2, 4, and 24 h) 10-μl aliquots were taken and quenched with 10 μl of 0.1 M NEM. The samples were then added to SDS-PAGE sample buffer, heated to 100 °C for 5 min, and analyzed by Western blotting. A zero time point was obtained by quenching an aliquot of the diluted membranes before addition of $CuCl_2$.

Analytical Ultracentrifugation—Analytical ultracentrifugation studies were conducted using a Beckman XL-A Analytical Ultracentrifuge. All studies were carried out at 20 °C in buffer containing 50 mM Tris-HCl, pH 8.0, 100 mM NaCl, and 1 mM EDTA. Sedimentation velocity runs were at 60,000 rpm. The data were analyzed with the Beckman software using both the transport method and the second moment method; essentially identical results were obtained. Sedimentation equilibrium studies were carried out at various rotor speeds ranging from 18,000 to 48,000 rpm. Equilibrium was ascertained by the coincidence of scans taken 2 h apart. Data were fitted to a model with a single ideal species. Partial specific volumes were calculated from the inferred amino acid compositions as described by Cohn and Edsall (25).

Other Procedures—SDS-PAGE was carried out as described by Laemmli (26), using 15% separating gels. The proteins were stained with Coomassie Brilliant Blue R-250. Blotting was carried out in carbonate blot buffer as described previously (27), onto polyvinylidene difluoride membranes. An anti-*b* monoclonal antibody, 10-1A4, was a generous gift of Karlheinz Altendorf and Gabriele Deckers-Hebestreit and was labeled with ^{125}I by the IODO-GEN method (28). N-terminal analysis using dansyl chloride was carried out as described by Gray (29). Electrospray mass spectrometry was carried out at the Biological Mass Spectrometry Laboratory at the University of Waterloo (Waterloo, Ontario) using a Quattro II triple quadrupole mass spectrometer (Micromass, UK) in the positive ion mode.

RESULTS

Construction of b_{syn} and Mutagenesis—The *b* subunit is an integral membrane protein, with a single membrane-spanning region at the N terminus. To facilitate study of this protein, the sequence encoding the entire subunit except for the N-terminal 24 amino acids has previously been subcloned into pUC8 to produce the plasmid pSD59; the polypeptide expressed has been called b_{sol} (10). To make the introduction of mutations into b_{sol} easier, a gene containing numerous silent mutations was designed such that useful restriction endonuclease sites were added. The gene was synthesized as eight overlapping oligonucleotides, which were assembled in the multiple cloning region of pUC8 to produce the plasmid pDM3. The encoded protein, named b_{syn}, has an eight-residue leader sequence (MTMIT-NSH) identical to b_{sol}, followed by the sequence of the *b* subunit starting at residue Tyr-24 (Fig. 1). b_{syn}, therefore, contains one additional residue relative to b_{sol}, but is otherwise identical; neither protein contains any cysteine residues. b_{syn} is soluble, is recognized by anti-*b* monoclonal antibodies (not shown), and behaves similarly to b_{sol} during purification.

Single cysteine mutations were introduced into the gene product at a variety of positions; two main regions were targetted for mutagenesis (Fig. 1). First, on the basis of the heptad repeat found from residues 33 to 79 of *b*, it has been previously suggested that this region adopts a coiled-coil structure (10, 30). To investigate this region, residues 59–65, representing one full cycle of the heptad repeat, as well as residue Ala-68, an additional heptad *d* position, have been mutated individually to cysteine (throughout this paper, all residue numbering is based on the full-length *E. coli b* sequence). Second, residue

```
                EcoRI      SnaBI                          MfeI
ATGACCATGATTACGAATTCCCACTACGTATGGCCACCATTAATGGCAGCAATTGAAAAG
 M  T  M  I  T  N  S  H  Y  V  W  P  P  L  M  A  A  I  E  K
                        24                   30

                                  NheI        BssHII    BglII
CGCCAAAAAGAAATTGCTGATGGCCTTGCTAGCGCGGAACGCGCGCATAAAGATCTTGAC
 R  Q  K  E  I  A  D  G  L  A  S  A  E  R  A  H  K  D  L  D
          40                                50

    EcoNI            BclI   AflII       StyI BspMI
CTCGCGAAGGCCAGCGCGACTGATCAGCTTAAGAAAGCCAAGGCGGAAGCGCAGGTAATC
 L  A  K  A  S  A  T  D  Q  L  K  K  A  K  A  E  A  Q  V  I
          60                                70

                                PflMI               Bpu10I
ATCGAGCAGGCCAACAAACGCCGCTCCCAGATTCTGGACGAAGCGAAAGCTGAGGCAGAA
 I  E  Q  A  N  K  R  R  S  Q  I  L  D  E  A  K  A  E  A  E
          80                                90

       BsiWI                                      Bpu102I
CAGGAACGTACGAAAATCGTTGCGCAGGCGCAGGCGGAAATTGAAGCTGAGCGTAAACGT
 Q  E  R  T  K  I  V  A  Q  A  Q  A  E  I  E  A  E  R  K  R
          100                               110

  PmlI                                SfiI           NgoAIV
GCACGTGAAGAGCTGCGTAAGCAAGTGGCCATCCTGGCCGTTGCCGGCGCCGAGAAGATC
 A  R  E  E  L  R  K  Q  V  A  I  L  A  V  A  G  A  E  K  I
          120                               130

    Eco47III HincII              EcoRV                  BanII
ATCGAGCGCTCCGTTGACGAAGCTGCTAACAGCGATATCGTAGATAAACTTGTCGCAGAG
 I  E  R  S  V  D  E  A  A  N  S  D  I  V  D  K  L  V  A  E
          140                               150

             HindIII
CTCTAACTAACTAAGCTT
 L  *
```

FIG. 1. **Nucleotide sequence of the synthetic gene encoding b_{syn}.** Restriction sites that are unique in the pDM3 plasmid are indicated. The amino acid sequence of b_{syn} is given *below* the DNA sequence; the 8-residue leader sequence is indicated in *italics*. Numbering is based on the full-length *b* subunit, starting at residue Tyr-24. Residues that were mutated to cysteine appear in *bold* type.

Ala-128 has been implicated in *b* dimerization interactions (15). Each residue in the "VAILAVA" region (positions 124–132) has also been mutated to cysteine to examine this region. In addition, three residues toward the C terminus were mutated (positions 138, 139, and 146). Note that since the b_{syn} polypeptide exists as a dimer in solution, the introduction of a single cysteine mutation into the gene results in the presence of two cysteines in the dimer. Throughout this paper we will refer to the position of the cysteine residue in one subunit as *n* and the position of the cysteine in the second subunit as *n′*.

Disulfide Bond Formation Near the C Terminus—One convenient method used to induce disulfide bond formation is incubation with excess glutathione (31, 32). Glutathione (GSH/GSSG) acts as a disulfide buffer and as a disulfide exchange reagent; after one cysteine residue forms a mixed disulfide with glutathione, a second nearby cysteine can displace it, forming a protein-protein disulfide bond. The second cysteine will not be able to react if it is too far away or has poor geometry for disulfide formation. Eventually an equilibrium is reached; if the disulfided form of the protein predominates at equilibrium, then one may infer that the two cysteines are close together. Equilibrium can be assumed if the same result is obtained regardless of whether the proteins started in a fully reduced or a fully oxidized state.

The glutathione procedure is illustrated for b_{syn} polypeptides containing cysteines in positions 128, 138, 139, or 146 (Fig. 2). The proteins were incubated with a glutathione mixture (GSSG/GSH = 1.1:1) as described under "Experimental Procedures." At various time points aliquots were reacted with excess NEM to modify all thiol groups present and thus prevent further disulfide exchange. Each polypeptide was reacted in duplicate, being either mostly oxidized or mostly reduced at the start of the experiment (Fig. 2*A*). Comparison of the band intensities after 2 h of incubation (Fig. 2*B*) revealed that equilibrium had been attained. The proteins containing the A128C and S139C mutations showed a strong tendency to dimerize,

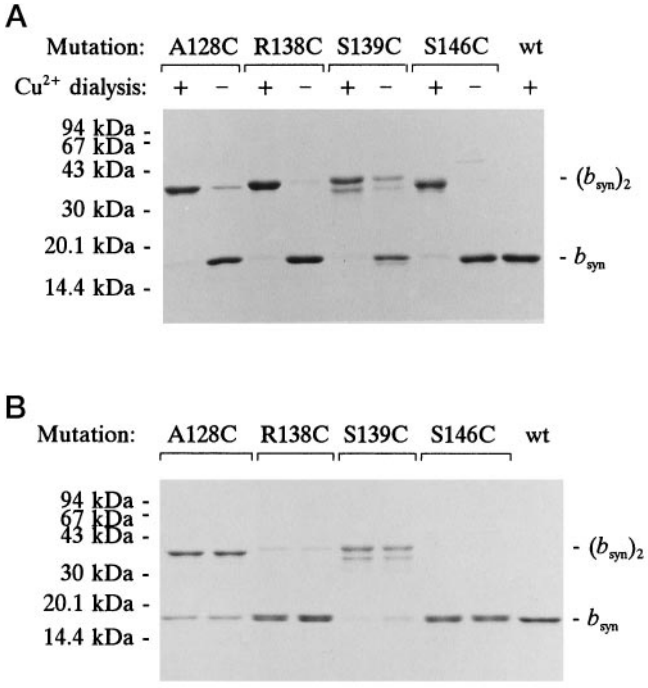

FIG. 2. **Disulfide bond formation induced by glutathione.** *Panel A*, purified b_{syn} proteins containing the mutations indicated, as well as the wild type, were dialyzed in a buffer containing either 10 μM $CuCl_2$ or 1 mM DTT to obtain oxidized or reduced proteins, respectively. Samples of each protein were quenched with NEM, added to sample buffer lacking reducing agent, and analyzed by SDS-PAGE. *Panel B*, in reactions carried out in parallel, the wild type control and the two dialyzed samples of each cysteine mutant protein were incubated in the presence of an excess of glutathione as described under "Experimental Procedures." After 2 h, the reactions were quenched with excess NEM and samples were analyzed by SDS-PAGE under nonreducing conditions.

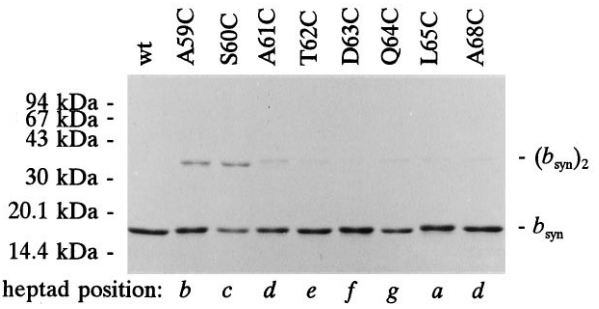

FIG. 3. **Disulfide bond formation in the heptad repeat region.** Purified b_{syn} proteins containing the mutations indicated were dialyzed in a buffer containing either 10 μM $CuCl_2$ or 1 mM DTT and treated with excess glutathione as described under "Experimental Procedures." After 2 h, the reactions were quenched with excess NEM and samples were analyzed by nonreducing SDS-PAGE. It was verified that the reactions had reached equilibrium (not shown); only the proteins that had been dialyzed in the presence of $CuCl_2$ (*i.e.* were oxidized before glutathione treatment) are shown here. The position of each mutation in the heptad repeat pattern is indicated.

while cysteines at positions 138 and 146 did not tend to form disulfides under these conditions. These results imply that positions 128 and 128′ are close together in the quaternary structure of the dimer, as are positions 139 and 139′, suggesting a parallel interaction between the b_{syn} subunits in this region. In contrast, cysteine residues at positions 138 and 138′ lack either proximity or proper orientation, as do the residues at 146 and 146′. It is evident from Fig. 2 that it is possible to observe a wide range of propensities for disulfide bond formation using this procedure. Note that because equilibrium was reached, the lack of disulfide formation at positions 138 and 146 cannot be due to inaccessibility of the residues to the glutathione.

Disulfide Formation within the Heptad Repeat Region—A similar experiment was performed with b_{syn} proteins containing mutations at positions 59–65 or 68 in the heptad repeat region; results are shown for samples which began in the fully oxidized form (Fig. 3). Of these positions, the A59C (heptad *b* position) and S60C (heptad *c* position) proteins showed the highest tendency to form disulfides; however, they did not form nearly as completely as the A128C or S139C proteins. Cysteines in the other heptad positions had poor propensities to form disulfides (Fig. 3). In a coiled-coil domain, cysteines at the *d* positions of the heptad repeat (residues 61 and 68) would be expected to show the highest tendency to form disulfide bonds, since such bonds at these positions perturb the residue orientation and secondary structure the least (33). The result that the *b* and *c* positions in this region of b_{syn} showed the highest propensities to form disulfide bonds is inconsistent with the presence of a coiled-coil structure, in which predominantly hydrophobic residues in the *a* and *d* positions form an interface.

Mixed Disulfide Formation in the Heptad Repeat Region—To investigate the relationship between the subunits of the b_{syn} dimer, proteins containing single cysteine mutations in the region 59–65 were mixed in pairs representing all possible combinations of two. Glutathione was added as described earlier, and the reactions were quenched with NEM after 2 h. Selected results are shown (Fig. 4); in most cases, mixed disulfide formation did not occur to an extent greater than that seen for the individual mutations by themselves (*e.g.* S60C + A61C, A61C + D63C, and D63C + L65C in Fig. 4). The highest level of disulfide formation was observed with the S60C + L65C and A61C + L65C combinations. Since the proteins were pure before they were mixed, this observation implies that exchange of subunits between b_{syn} dimers must have taken place during the course of the reaction. In addition, the result suggests that residue 65 of one subunit is close to residues 60 and 61 of the other, while other combinations of positions in this region are not as close or of correct geometry for disulfide bond formation.

Cu^{2+}-catalyzed Disulfide Bond Formation—Air oxidation catalyzed by Cu^{2+} (34, 35) was selected as a complementary method of gauging tendencies to form disulfide bonds. For this technique the proteins of interest were first dialyzed in the presence of 1 mM DTT; the dialysis bags were then transferred to an open beaker of buffer containing 10 μM $CuCl_2$ and 10 mM free cysteine. The formation of intersubunit disulfide bonds was then followed over a 48-h period by periodically quenching aliquots of the samples with NEM followed by non-reducing SDS-PAGE. Analysis by this method, when applied to a number of mutations examined in Figs. 2 and 3, produced results consistent with those obtained by incubation with glutathione (data not shown).

The Cu^{2+} dialysis technique was used to test partially purified b_{syn} proteins carrying single cysteine mutations in positions 124–132 or in position 138 (Fig. 5). At the zero time point, after dialysis in the presence of DTT, the b_{syn} proteins were completely reduced (Fig. 5*A*). After 2 h of dialysis in the presence of 10 μM $CuCl_2$ and 10 mM free cysteine, the most complete disulfide bond formation was observed at positions 124, 128, and 132 (Fig. 5*B*); the relative levels of oxidation did not change significantly upon further dialysis (not shown). The 4-residue periodicity of cross-linking is striking and suggests a parallel α-helical arrangement in this region.

Disulfide Bond Formation in Membrane-bound b—The full-length *b* subunit carrying either the R138C or the S139C mutation was expressed from a plasmid in cells of strain KM2, which has a chromosomal deletion of the *uncF* gene (18). The

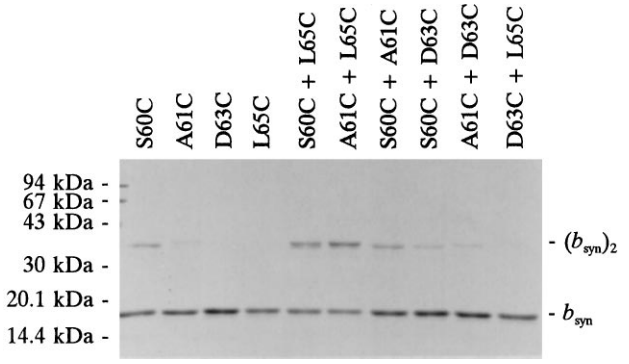

FIG. 4. **Mixed disulfide formation in the heptad repeat region.** Purified b_{syn} proteins containing cysteine mutations were dialyzed in a buffer containing 1 mM DTT or 10 μM $CuCl_2$ and then mixed in the combinations indicated. The mixtures were treated with excess glutathione as described under "Experimental Procedures." After 2 h, the reactions were quenched with excess NEM and samples were analyzed by nonreducing SDS-PAGE. It was verified that the reactions had reached equilibrium (not shown); only the proteins that had been dialyzed in the presence of DTT (*i.e.* were reduced before glutathione treatment) are shown here.

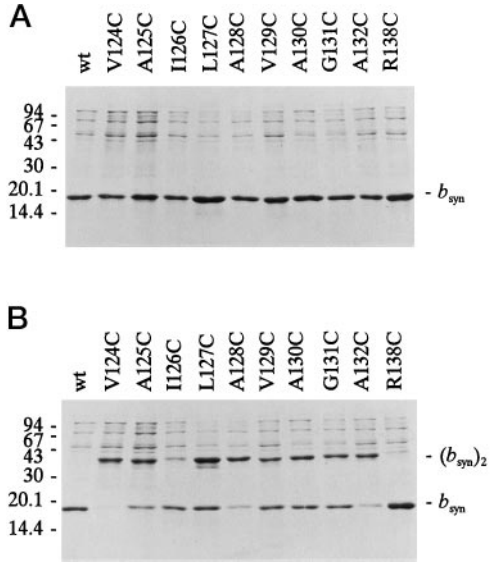

FIG. 5. **Disulfide bond formation in the VAILAVA region.** Partially purified b_{syn} proteins containing the mutations indicated were dialyzed in a buffer containing 1 mM DTT. Samples were quenched with NEM and analyzed by nonreducing SDS-PAGE (*panel A*). The proteins were then dialyzed against a buffer containing 0.1 M $NaHCO_3$, 10 μM $CuCl_2$, and 10 mM cysteine for 2 h (*panel B*) before quenching with NEM.

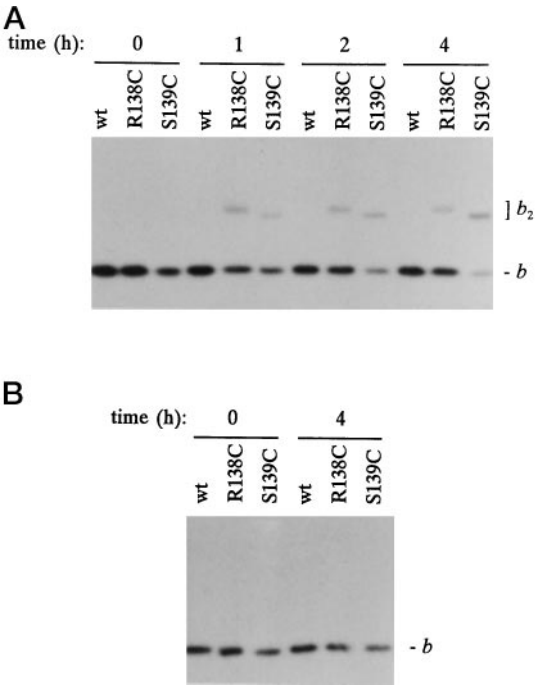

FIG. 6. **Disulfide formation in membrane-bound *b*.** 1100, KM2/pDM112, and KM2/pDM113 cells were induced and membrane preparations were made as described under "Experimental Procedures." The membranes were treated with 10 μM $CuCl_2$ and aliquots were quenched with NEM after 1, 2, and 4 h. SDS-PAGE sample buffer was added and the samples were analyzed by Western blotting using ^{125}I-labeled monoclonal antibody 10-1A4. The zero time point was obtained by quenching samples with NEM before addition of $CuCl_2$. *Panel A*, no DTT was added to the samples; *panel B*, 0.1 M DTT was added before analysis.

level of induction was such that the amount of *b* expressed from the plasmids was almost the same as that expressed from the chromosome of 1100 cells, as analyzed by Western blotting (data not shown). Membranes from these cells were prepared such that the F_1F_0-ATPase complex should remain intact, and were then treated with 10 μM $CuCl_2$. At various times, aliquots were quenched with NEM and analyzed by Western blotting (Fig. 6*A*). The wild type *b* subunit contains one cysteine residue (Cys-21), but this residue did not form disulfides under these conditions (Fig. 6*A*). Some disulfide formation was observed in the R138C protein after only 1 h of incubation, but the level of dimer did not increase with time. The S139C protein showed a consistent increase in the amount of disulfide formed, with most of the protein in the disulfided state after 4 h of incubation. To investigate the loss of signal in the S139C protein with increasing time, the samples were reduced with DTT and blotted again (Fig. 6*B*). After reduction, the intensity of the S139C band returned to its original level, implying that the antibody used does not recognize the disulfide-bonded form as efficiently as the monomer. Thus it is likely that the actual ratio of oxidized:reduced S139C in Fig. 6*A* is higher than is apparent from the relative band intensity. A 9.5-fold longer exposure of the blot shown in Fig. 6*A* revealed no cross-linking of *b* to any other proteins (data not shown). When the membranes were incubated with a 1.1:1 ratio of GSSG:GSH, or with 10 μM $CuCl_2$ and 10 mM cysteine, no disulfide bonds were observed (data not shown).

Sedimentation Analysis of b_{syn} and N-terminal Truncations—Previously we reported the characterization of b_{sol} as a 31-kDa dimer by sedimentation equilibrium analysis (10). This has been confirmed with b_{syn}, but we have observed that inclusion of data up to an A_{280} of 0.8, which corresponds to a protein concentration of 1.6 mg/ml, resulted in an apparent molecular weight of 34,200 and a pattern of residuals indicative of aggregates at higher concentrations (data not shown). In contrast, analysis of nine data sets which were limited to concentrations below 0.7 mg/ml gave an average molecular weight of 30,600 (Table I) and random patterns of residuals.

Plasmids encoding three forms of the protein with additional residues deleted from the N terminus were constructed as described under "Experimental Procedures." In protein b_{34-156}, the hydrophobic sequence $Y^{24}VWPPLMAAI^{33}$ was removed and a different leader sequence, MSYW, was placed before residues Glu-34 to Leu-156 to provide optical absorbance at 280 nm (the *b* sequence contains no aromatic residues after Trp-26). The same leader was also placed at the N terminus of protein b_{53-156}, which lacked both the hydrophobic sequence noted above and also the first portion of the heptad repeat sequence in the polar domain. Both of these proteins behaved

TABLE I
Sedimentation analysis of b_{sys} and N-terminal truncations

Protein	Sequence[a]	Partial specific volume,[a] ν	Polypeptide molecular weight[a]	Observed molecular weight[b]	Sedimentation coefficient,[c] $s_{20,w}$	Frictional ratio,[d] f/f_{min}
b_{syn}	$TMITNSHY^{24}$–L^{156}	0.740	15,509	30,600 ± 2000; n = 9	1.80S	1.87
b_{34-156}	$SYWE^{34}$–L^{156}	0.739	14,018	27,800 ± 1500; n = 8	1.81S	1.74
b_{53-156}	$SYWD^{53}$–L^{156}	0.742	11,899	25,300 ± 1000; n = 8	1.70S	1.63
b_{67-156}	$(SYWL^{65}K^{66})K^{67}$–L^{156}	0.745	9,991	10,200 ± 530; n = 6	0.96S	1.61

[a] Removal of the initiating methionine residue was assumed for all proteins. Residues in parentheses were removed during purification and were excluded from calculations.
[b] Sedimentation equilibrium data for b_{syn} were obtained at a rotor speed of 30,000 rpm and initial protein concentrations of 0.48, 0.24, and 0.12 mg/ml; data sets were selected such that the maximal absorbance corresponded to a protein concentration of less than 0.75 mg/ml. Data for b_{34-156} and b_{53-156} were obtained at rotor speeds of 18,000, 25,000, and 30,000 rpm with an initial protein concentration of 0.2 mg/ml; data sets were selected such that the maximal absorbance corresponded to a protein concentration of less than 0.66 mg/ml (b_{34-156}) or 0.56 mg/ml (b_{53-156}). Data for b_{67-156} were obtained at 241 nm using rotor speeds of 42,000 and 48,000 rpm with an initial protein concentration of 0.66 mg/ml; data up to a concentration of 2.9 mg/ml were included in analyses. Data were fit using a single component model, and are presented as the average ± S.E.; n, number of determinations.
[c] Protein concentrations in sedimentation velocity experiments were 1.0 mg/ml for b_{syn} and b_{34-156}, 0.85 mg/ml for b_{53-156}, and 0.82 mg/ml for b_{67-156}. The latter protein was observed at 235 nm. Values presented were calculated using the second moment method.
[d] Frictional ratios were calculated using molecular weights of 31,018 for b_{syn}, 28,036 for b_{34-156}, 23,798 for b_{53-156}, and 9,991 for b_{67-156}.

similarly to b_{syn} during purification and both existed as dimers at relatively low concentrations (Table I), while slight aggregation was observed at higher concentrations (data not shown).

The sedimentation coefficients of the proteins were determined in sedimentation velocity experiments at 20 °C, corrected to pure water, and used to calculate frictional ratios by standard methods. Clearly, removal of the N-terminal sequence caused the protein to become less asymmetric, although a frictional ratio of 1.63 is still high for a globular protein.

The precursor of protein b_{67-156} was expressed with the same leader as b_{34-156} and b_{53-156}, but its behavior and properties were quite different. Absorbance at 280 nm was lost during purification, indicating proteolytic removal of the entire leader sequence from the N terminus. The molecular weight of the purified polypeptide was determined by electrospray mass spectrometry to be 9,989.6, and N-terminal analysis by dansylation identified lysine, indicating that residues Leu-65 and Lys-66 had also been removed, leaving Lys-67 as the N terminus (expected molecular weight, 9,991.4). Sedimentation equilibrium analysis revealed this protein to be monomeric even at relatively high concentrations.

DISCUSSION

Our results do not support a coiled-coil model for residues 33–79 of *b*. Upon incubation with glutathione the A59C and S60C mutations formed disulfides more readily than any other position tested in the heptad repeat region (Fig. 3). These residues occupy positions *b* and *c* of the heptad repeat; therefore in a standard coiled-coil they would be on opposite sides of the helices and would not be expected to form disulfides easily. At the same time, the two *d* position sites tested (mutations A61C and A68C) showed little tendency to form disulfides. In addition, the sedimentation equilibrium ultracentrifugation experiments with N-terminal truncations imply that residues 53–66 are critical for b_{syn} dimer formation, but that residues 24–52 are not (Table I). If a coiled-coil structure were present, one would expect a gradual shift from dimer toward monomer rather than the abrupt transition caused by removal of residues 53–66. Therefore both the disulfide formation and the sedimentation equilibrium results are inconsistent with the presence of a coiled-coil structure between residues 33–68 of the *b* subunit.

Interestingly, at none of the positions between 59 and 68 did disulfide bond formation occur to the extent observed for several mutations toward the C terminus (*e.g.* 124, 128, and 139). This result, as well as the observation that disulfide formation at position 60 does not readily occur in the F_1F_0 complex,[2] raises the question of whether or not positions 59 and 60 actually form tight interactions in the dimer. It seems possible that the residues could be spatially close but not tightly interacting; if so, the molecular dynamics of protein structure might frequently bring the cysteines into correct orientation for disulfide formation in b_{syn}.

When proteins containing cysteine residues at different positions were mixed, the strongest disulfide formation occurred between positions 60 and 65′, and positions 61 and 65′ (Fig. 4). The fact that disulfide formation occurred to a greater extent in the mixtures than in the pure proteins implies exchange between b_{syn} dimers, and therefore the establishment of a monomer/dimer equilibrium. This equilibrium seems to lie strongly in favor of the dimeric form, as evidenced by the ultracentrifugation data. Also, the ability of residues 60 and 61 to form disulfides with residue 65′ more strongly than with their counterparts in the opposing subunit suggests that some structure other than simple parallel and symmetrical α-helices (as would be the case in a coiled-coil structure) exists in this region. It is possible that a single helix is present in each dimer, but that these helices are staggered relative to each other; alternatively a less regular structure or a turn may be present between residues 61 and 65.

Among the more C-terminal mutations, disulfide bond formation was strongest at positions 128 and 139 in the glutathione reactions (Fig. 2), and at positions 124, 128, and 132 in the air oxidation experiments (Fig. 5). These results imply that the *b* subunits interact in a parallel fashion in this region with, for example, the residue in position 124 closely interacting with the residue in position 124′. Furthermore, the periodic nature of disulfide bond formation propensities between residues 124 and 132 suggests that two interacting parallel α-helices exist in this region. It is especially noteworthy that, among bacterial and chloroplast *b* subunits, positions 124, 128, and 132 are well conserved (36). When the residues in this region were mutated individually to aspartate, a similar periodic effect on bacterial growth yield and ATPase activity was observed (15).

The results obtained with the soluble b_{syn} protein are supported by the experiment using the entire *b* subunit in membranes, in which R138C showed a poor tendency to form disulfides while S139C formed disulfides well (Fig. 6). Because R138C disulfide formation achieved its maximal, but low, level after 1 h (Fig. 6*A*), it is possible that the disulfided protein

[2] A. J. W. Rodgers, R. Aggeler, M. B. Morris, R. A. Capaldi, and S. M. Howitt, unpublished data.

represents a minor fraction of *b* subunits that were not properly incorporated into the ATPase complex.

The strong tendency of residue 139 to form disulfides, coupled with the similar behavior of cysteines at positions 124, 128, and 132, suggests that an α-helix may extend from residue 124 to 139, forming an important dimerization interface between the subunits. There are hydrophobic residues (isoleucines) at positions 135 and 136 of the *E. coli* subunit (Fig. 1); position 136 is hydrophobic in almost all of the species listed by Blair *et al.* (36). Therefore such a helix would have a relatively hydrophobic face that could interact with the corresponding residues on the other *b* subunit. While we did not observe disulfide bond formation in b_{syn} at position 146, which would lie on the same face of this proposed helix, Rodgers *et al.*[2] found a disulfide at this position to form relatively readily in F_1F_0. These results imply that a conformational change occurs in this region upon the binding of *b* to F_1.

Previously, Howitt *et al.* (15) observed that an A128D mutation caused reduction of ATPase activity in membranes as well as loss of dimerization of their soluble *b* protein. Our present results indicate that the 128 and 128′ positions are close together in the b_{syn} dimer, and therefore it is likely that the effects of the A128D mutation are due to mutual repulsion of the like-charged residues incorporated at a key interaction site. A similar explanation likely holds true for the observation that a G131D mutation in *b* prevents proper assembly of the F_1F_0 complex (14).

The present studies shed substantial new light on the structure of the *b* subunit. Soluble forms of *b* that lack the transmembrane region form dimers with extended and mostly α-helical structures (10, 15). On the basis of the fact that a single mutation (A128D) is able to abolish dimerization of the hydrophilic portion of *b*, it has been suggested that interactions in the hydrophilic domain are not important in dimerization in the wild type *b* subunit (9). An end-to-end, rather than a side-by-side, orientation of the soluble dimer was proposed. Furthermore, a model for the structure of *b* was presented in which the N-terminal transmembrane helices are closely associated but the hydrophilic regions extend away from each other (9). In contrast, the work presented here implies that residues in regions 53–66 and 124–139 are involved in b_{syn} dimer formation, and therefore that dimerization interactions depend on residues distributed throughout the soluble subunits. A model in which a pair of long α-helices extend in parallel toward F_1 from the membrane is attractive, especially in light of the steadily decreasing frictional ratios observed upon removal of residues between Val-25 and Asp-53 (Table I), and yet our present results argue against association of these helices in a coiled-coil structure. The C-terminal region appears to form a more globular structure, possibly centered around hydrophobic core helices between residues 124 and 132. Residues in this putative globular domain would provide important dimerization contacts, as well as sites of interaction with F_1.

Proteolysis studies have revealed that the hydrophilic portion of the *b* subunit is required for binding of F_1 to the membrane (11–13). Cryo-electron microscopy using b_{sol} and F_1 have implied that *b* interacts with the C-terminal domain of one of the β subunits of F_1 (37). These observations suggest that *b* may play a role in energy coupling between proton translocation in F_0 and ATP synthesis in F_1. In future studies it will be important to further explore areas of contact between *b* and F_1, as these interactions may give insight as to the functional role played by *b* in the intact complex.

Acknowledgments—We thank Faye Males for expert technical assistance, Drs. Karlheinz Altendorf and Gabriele Deckers-Hebestreit for providing the 10-1A4 monoclonal antibody, Drs. Kimberly McCormick and Brian Cain for providing strain KM2, and Kim Kawamura for constructing plasmid pKK1.

REFERENCES

1. Fillingame, R. H. (1997) *J. Exp. Biol.* **200,** 217–224
2. Deckers-Hebestreit, G., and Altendorf, K. (1996) *Annu. Rev. Microbiol.* **50,** 791–824
3. Nakamoto, R. K., and Futai, M. (1996) in *Biomembranes* (Lee, A. G., ed) Vol. 5, pp. 343–367, Jai Press, Greenwich, CT
4. Boyer, P. D. (1993) *Biochim. Biophys. Acta* **1140,** 215–250
5. Schneider, E., and Altendorf, K. (1987) *Microbiol. Rev.* **51,** 477–497
6. Vik, S. B., and Antonio, B. J. (1994) *J. Biol. Chem.* **269,** 30364–30369
7. Duncan, T. M., Bulygin, V. V., Zhou, Y., Hutcheon, M. L., and Cross, R. L. (1995) *Proc. Natl. Acad. Sci. U. S. A.* **92,** 10964–10968
8. Cox, G. B., Fimmel, A. L., Gibson, F., and Hatch, L. (1986) *Biochim. Biophys. Acta* **849,** 62–69
9. Howitt, S. M., Rodgers, A. J. W., Hatch, L. P., Gibson, F., and Cox, G. B. (1996) *J. Bioenerg. Biomembr.* **28,** 415–420
10. Dunn, S. D. (1992) *J. Biol. Chem.* **267,** 7630–7636
11. Hermolin, J., Gallant, J., and Fillingame, R. H. (1983) *J. Biol. Chem.* **258,** 14550–14555
12. Hoppe, J., Friedl, P., Schairer, H. U., Sebald, W., von Meyenburg, K., and Jørgensen, B. B. (1983) *EMBO J.* **2,** 105–110
13. Perlin, D. S., Cox, D. N., and Senior, A. E. (1983) *J. Biol. Chem.* **258,** 9793–9800
14. Jans, D. A., Hatch, L., Fimmel, A. L., Gibson, F., and Cox, G. B. (1985) *J. Bacteriol.* **162,** 420–426
15. Howitt, S. M., Rodgers, A. J. W., Jeffrey, P. D., and Cox, G. B. (1996) *J. Biol. Chem.* **271,** 7038–7042
16. Sambrook, J., Fritsch, E. F., and Maniatis, T. (1989) *Molecular Cloning: A Laboratory Manual,* 2nd Ed., Cold Spring Harbor Laboratory Press, Cold Spring Harbor, NY
17. Messing, J., Crea, J., and Seeburg, P. H. (1981) *Nucleic Acids Res.* **9,** 309–321
18. McCormick, K. A., and Cain, B. D. (1991) *J. Bacteriol.* **173,** 7240–7248
19. Vieira, J., and Messing, J. (1982) *Gene* (*Amst.*) **19,** 259–268
20. McLachlin, D. T., and Dunn, S. D. (1996) *Protein Expression Purif.* **7,** 275–280
21. Smith, S. P., Barber, K. R., Dunn, S. D., and Shaw, G. S. (1996) *Biochemistry* **35,** 8805–8814
22. Walker, J. E., Saraste, M., and Gay, N. J. (1984) *Biochim. Biophys. Acta* **768,** 164–200
23. Bradford, M. M. (1976) *Anal. Biochem.* **72,** 248–254
24. Lowry, O. H., Rosebrough, N. J., Farr, A. L., and Randall, R. J. (1951) *J. Biol. Chem.* **193,** 265–275
25. Cohn, E. J., and Edsall, J. T. (1943) *Proteins, Amino Acids, and Peptides*, pp. 157–161, Reinhold, New York
26. Laemmli, U. K. (1970) *Nature* **227,** 680–685
27. Dunn, S. D. (1986) *Anal. Biochem.* **157,** 144–153
28. Fraker, F. J., and Speck, J. C. (1978) *Biochem. Biophys. Res. Commun.* **80,** 849–857
29. Gray, W. R. (1972) *Methods Enzymol.* **25,** 121–138
30. McCormick, K. A., Deckers-Hebestreit, G., Altendorf, K., and Cain, B. D. (1993) *J. Biol. Chem.* **268,** 24683–24691
31. Gilbert, H. F. (1995) *Methods Enzymol.* **251,** 8–28
32. Creighton, T. E. (1984) *Methods Enzymol.* **107,** 305–329
33. Zhou, N. E., Kay, C. M., and Hodges, R. S. (1993) *Biochemistry* **32,** 3178–3187
34. Takagi, T., and Isemura, T. (1964) *J. Biochem.* **56,** 344–350
35. Ahmed, A. K., Schaffer, S. W., and Wetlaufer, D. B. (1975) *J. Biol. Chem.* **250,** 8477–8482
36. Blair, A., Ngo, L, Park, J., Paulsen, I. T., and Saier, M. H. (1996) *Microbiology* **142,** 17–32
37. Wilkens, S., Dunn, S. D., and Capaldi, R. A. (1994) *FEBS Lett.* **354,** 37–40

Dimerization Interactions of the *b* Subunit of the *Escherichia coli* F_1F_0-ATPase

Derek T. McLachlin and Stanley D. Dunn

J. Biol. Chem. 1997, 272:21233-21239.
doi: 10.1074/jbc.272.34.21233